JACC: BASIC TO TRANSLATIONAL SCIENCE VOL. 9, NO. 2, 2024


ORIGINAL RESEARCH - PRECLINICAL

# Epicardial CCM2 Promotes Cardiac Development and Repair Via its Regulation on Cytoskeletal Reorganization

Rui Wang, PhD,[a,b,*] Dongbo Lu, BS,[a,*] Renhua Song, PhD,[c] Luping Du, PhD,[d] Xi Yang, PhD,[a] Shi-ting Wu, PhD,[a] Xiaohong Wang, PhD,[a] Justin Wong, PhD,[c] Zhelong Xu, MBBS, PhD,[d] Qiang Zhao, PhD,[e] Renjing Liu, PhD,[f] Xiangjian Zheng, PhD[a]

## VISUAL ABSTRACT

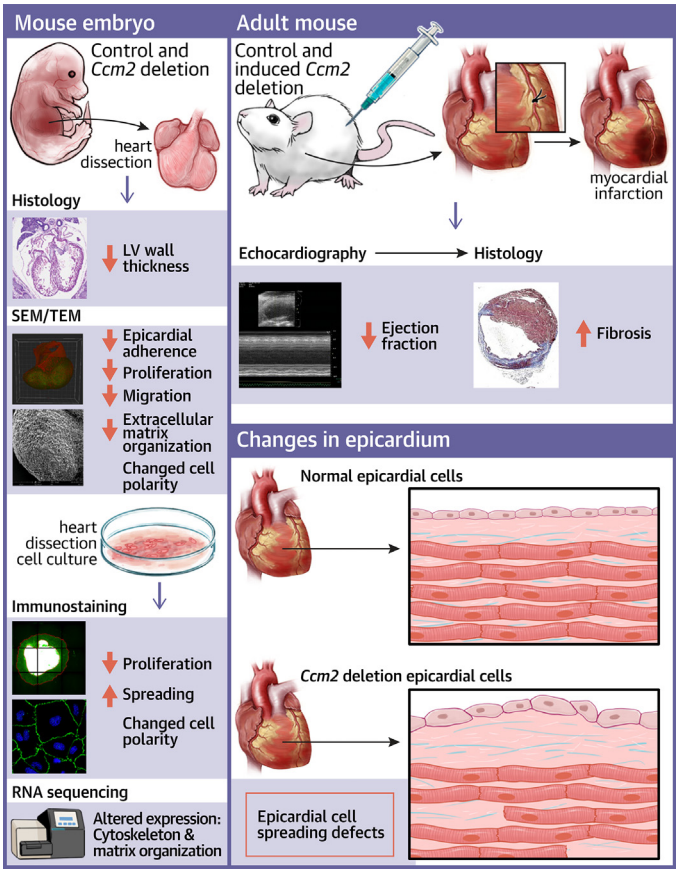


Wang R, et al. J Am Coll Cardiol Basic Trans Science. 2024;9(2):203-219.

## HIGHLIGHTS

- **CCM2 is a new signaling molecule in epicardium for heart development.**
- **In vivo analysis and ex vivo culture of epicardial cells demonstrated a cell autonomous role of Ccm2 in epicardial cells and contributes to cardiac development and repair.**
- **CCM2 controls cell shape and migration by regulating the expression of cytoskeletal and matrix genes.**

ISSN 2452-302X https://doi.org/10.1016/j.jacbts.2023.09.004

**ABBREVIATIONS AND ACRONYMS**

**CCM** = cerebral cavernous malformation

**EPDC** = epicardium derived cell

**Has1** = hyaluronan synthase 1

**MI** = myocardial infarction

**SUMMARY**

The epicardium provides epicardial-derived cells and molecular signals to support cardiac development and regeneration. Zebrafish and mouse studies have shown that *ccm2*, a cerebral cavernous malformation disease gene, is essential for cardiac development. Endocardial cell-specific deletion of *Ccm2* in mice has previously established that Ccm2 is essential for maintenance of the cardiac jelly for cardiac development during early gestation. The current study aimed to explore the function of Ccm2 in epicardial cells for heart development and regeneration. Through genetic deletion of *Ccm2* in epicardial cells, our in vivo and ex vivo experiments revealed that *Ccm2* is required by epicardial cells to support heart development. Ccm2 regulates epicardial cell adhesion, cell polarity, cell spreading, and migration. Importantly, the loss of *Ccm2* in epicardial cells delays cardiac function recovery and aggravates cardiac fibrosis following myocardial infarction. Molecularly, Ccm2 targets the production of cytoskeletal and matrix proteins to maintain epicardial cell function and behaviors. Epicardial Ccm2 plays a critical role in heart development and regeneration via its regulation of cytoskeleton reorganization. (J Am Coll Cardiol Basic Trans Science 2024;9:203-219) 

Ischemic heart disease remains the leading cause of death worldwide.[1,2] Detailed knowledge of the maturation steps presented by various cell types in the developing heart is key to achieving a proper understanding of cardiovascular development. The epicardium is the outer mesothelial layer of the heart and plays a crucial role in both embryonic heart development and adult heart repair.[3-5] During development, the epicardium sustains the underlying myocardium through paracrine signals that promote its growth. It is also an important cell source for myocardium during embryogenesis. Epicardium-derived cells (EPDCs) differentiate into cardiac fibroblasts, coronary smooth muscle cells, and potentially other cell types.[5-7] Upon cardiac injury, the epicardium is activated, undergoing proliferation and secreting cytokines that stimulate cardiomyocyte cell cycle re-entry.[5] The epicardium thus plays key roles in heart development and regeneration.

Decades of research have revealed that extracellular signals (such as TGF-β, retinoic acids, PDGF, FGF, and Hippo), and intracellular factors (such as Wt1, Tcf21, Cdc42, and NMIIB), regulate epicardial function.[8-16] The significance of cytoskeletal dynamics and extracellular matrix deposition in the epicardium has been less frequently addressed.

Cerebral cavernous malformations (CCMs) are sporadic or autosomal dominantly inherited vascular malformations in the brain.[17,18] The loss-of-function mutations in 3 genes, *CCM1, CCM2,* and *CCM3*, have been identified to cause human CCMs.[19-22] The role of CCM signaling in the developing heart was revealed in zebrafish studies, which showed that loss-of-function mutations in *ccm1, ccm2,* and *ccm3* resulted in a characteristic dilated heart phenotype.[23,24] Endocardial CCM regulates the MEKK3-KLF-ADAMTS signaling pathway to control endothelial gene expression during cardiovascular development. Loss of CCM signaling in endocardial cells resulted in the arrest of heart development associated with premature degradation of the cardiac jelly.[25] However, a role of CCM signaling in the epicardium has not been explored, and the molecular events of epicardial CCM signaling underlying heart development remain unknown.

This study aims to identify the role of CCM2 in heart development and regeneration. We analyzed

From the [a]Department of Pharmacology and Tianjin Key Laboratory of Inflammation Biology, School of Basic Medical Sciences, Tianjin Medical University, Tianjin, China; [b]Department of Microbiology, School of Medical Laboratory, Tianjin Medical University, Tianjin, China; [c]Epigenetics and RNA Biology Program, Centenary Institute and Sydney Medical School, The University of Sydney, Sydney, New South Wales, Australia; [d]Department of Physiology and Pathophysiology, School of Basic Medical Sciences, Tianjin Medical University, Tianjin, China; [e]Key Laboratory of Bioactive Materials (Ministry of Education), Frontiers Science Center for Cell Responses, College of Life Sciences, Nankai University, Tianjin, China; and the [f]Vascular Epigenetics Laboratory, Victor Chang Cardiac Research Institute and School of Clinical Medicine, Faculty of Medicine and Health, University of New South Wales, Sydney, New South Wales, Australia. *Drs Rui Wang and Lu contributed equally to this work as joint first authors.
The authors attest they are in compliance with human studies committees and animal welfare regulations of the authors' institutions and Food and Drug Administration guidelines, including patient consent where appropriate. For more information, visit the Author Center.

Manuscript received January 3, 2023; revised manuscript received September 8, 2023, accepted September 11, 2023.

the phenotypes of epicardial-specific *Ccm2*-deficient mice at different developmental stages. *Wt1*-Cre-mediated epicardial deletion of *Ccm2* led to embryonic lethality during midgestation. Histological analysis of epicardial *Ccm2*-deficient hearts at E12.5 revealed a thin myocardium and cardiac noncompaction compared with littermate control subjects. By employing gene expression analysis and immunohistochemistry approaches, we demonstrated that deletion of *Ccm2* impaired epicardial cell adhesion, proliferation, differentiation, and migration. Ex vivo cultures of epicardial cells from early gestation hearts revealed that Ccm2 plays a crucial role in regulating the expression of genes involved in cytoskeletal organization and matrix assembly, which are necessary for the maintenance of epicardial cell shape and polarity. Loss of epicardial-specific Ccm2 hindered cardiac regeneration following injury caused by increased fibrosis. Collectively, our study identifies epicardial-specific *Ccm2* as an essential gene for maintaining the integrity of the epicardium and its adhesion to the myocardium, which is required for heart development and injury repair.

## METHODS

**ANIMALS.** The $Wt1^{GFPCre/+}$, $Wt1^{ERT2Cre}$, $Ccm2^{fl/fl}$, and $Ccm3^{fl/fl}$ mice have been previously described.[26-29] All experimental animals were maintained on a 129/C57BL/6J mixed genetic background. The Institutional Animal Care and Use Committee of Tianjin Medical University approved all animal ethics and protocols. All experiments were conducted under the guidelines/regulations of Tianjin Medical University and the National Institutes of Health Guide for the Care and Use of Laboratory Animals.[30] For all experiments requiring animal tissues, tissues were harvested after animals were sacrificed with $CO_2$ inhalation in a euthanasia chamber followed with cervical dislocation.

**HISTOLOGY AND IMMUNOFLUORESCENCE STAINING.** The mouse embryos or hearts were collected in phosphate-buffered saline (PBS) and directly immersed in 4% paraformaldehyde in PBS (pH 7.4) overnight, embedded in paraffin, and sectioned. For immunostaining, sections were stained with rabbit anti-Wt1 (ab89901; Abcam; 1:500 dilution), EdU, Pdgfrα (AF1062; R&D; 1:100 dilution), Snail (3879; Cell Signaling Technology; 1:100 dilution), MF-20 (AB2147781; Developmental Studies Hybridoma Bank; 1:200 dilution), β-cantenin (sc-7963; SantaCruz; 1:300 dilution), ZO-1 (61-7300; Invitrogen; 1:100 dilution), Podoplanin (ab256559; Abcam; 1:300 dilution), GM130 (560066; BD Biosciences; 1:100 dilution), Phalloidin (F432; Invitrogen; 1:40 dilution), Krt19 (ab133496; Abcam; 1:500 dilution), α-tubulin (2125; Cell Signaling Technology; 1:50 dilution), Laminin (L9393; Sigma-Aldrich; 1:30 dilution), ColVI (ab182744; Abcam; 1:500 dilution), and GFP (ab6673; Abcam; 1:500 dilution). Imaging was performed using a Zeiss Axio-Imager_LSM-800 confocal microscope (Carl Zeiss).

**WHOLE EMBRYONIC HEART IMMUNOFLUORESCENCE STAINING.** Whole embryonic hearts were stained as described.[31] Briefly, whole embryos were fixed overnight in 4% paraformaldehyde. Dissected hearts were serially dehydrated through 5-minute changes with 25%, 50%, 75%, and 100% methanol, then they were rehydrated for 10 minutes in 75%, 50%, and 25% methanol. Whole hearts were permeabilized and blocked for 2 hours in PBS-MT (0.5% Triton 100x, 2% milk), and then incubated with primary antibody for 24 hours. After 3 washes, the embryos were incubated with secondary antibody for 24 hours, followed by 3 more washes with PBS-MT. After staining, hearts were cleared via Scale U (urea 4M, 30% glycerol, 0.1% Triton 100×) and then 3-dimensionally imaged. Z-stack images were acquired using a Zeiss Axio-Imager_LSM-800 confocal microscope. Three-dimensional images were reconstructed using Imaris software (version x64 9.0.1).

**EPICARDIAL CELL CULTURE SYSTEM.** Epicardial explants were prepared from E12.5 mouse hearts with the atria and outflow tract removed. The hearts were placed on 12 precoated well plates using M199 with penicillin-streptomycin, with the dorsal surface placed on the plate surface. Briefly, hearts were incubated on the plate for 30 minutes at 37 °C to allow the heart to adhere. One drop of prewarmed M199 medium with 5% fetal bovine serum was then added onto each heart section. The epicardial cells were allowed to grow for 24 hours.

For pharmacologic experiments, E12.5 mouse hearts were placed on transwells in 12 well plates. The M199 media were supplemented with 5% fetal bovine serum and 4-methylumbelliferone (4-MU) (500 μmol/L, MCE), or rBMP10 (100 ng/mL , LMAI). Medium (400 μL) was added to the plate wells and 200 μL medium was added to the insert wells. After 30 minutes, additional medium was added to transwells to cover the mouse hearts, and they were incubated for 24 hours.

**POLARITY INDEX CALCULATION.** Cell polarity analysis was performed as previously described.[32,33] Images were obtained by confocal microscope (LSM 800, Carl Zeiss) and analyzed by ImageJ software (1.51S, National Institutes of Health). To quantify cell

polarity, images of epicardial cells were stained with Golgi and nuclear markers. Leader cells were identified as the first row of cells on the front edge, and the follower cells comprised the second to third rows of cells away from the edge. The polarity of each cell was defined as the angle (α) between the Golgi-nuclei axis and the edge line. The polarity index was calculated using the following formula:

$$PI = \sqrt{\left(\frac{1}{N}\sum_{1}^{N} cos\ \alpha\right)^2 + \left(\frac{1}{N}\sum_{1}^{N} sin\ \alpha\right)^2}$$

**QUANTIFICATION OF EPICARDIAL CELLS POLARITY.** The angle between epicardial cells was measured and compared at E12.5. The clockwise direction was defined as the positive direction. The orientation of epicardial cells was determined using GM130, and the angle was measured between orientation of epicardial cells and the adjacent myocardial plain in the positive direction.

**SCAN ELECTRON MICROSCOPY AND TRANSVERSE ELECTRON MICROSCOPY.** For scanning electron microscopy, embryonic hearts were fixed overnight (2% paraformaldehyde, 2.5% glutaraldehyde in 0.1 mol/L cacodylate buffer), postfixed for 2 hours (1% osmium tetroxide, 0.8% potassium ferrocyanide in 0.1 mol/L phosphate buffer), and subsequently processed as described using standard protocols. Images were taken on a Phenom ProX Desktop Scanning Electron Microscope.

For transmission electron microscopy, embryonic hearts were processed as described for scanning electron microscopy until postfixation. Hearts were then dehydrated in a graded series of ethanol and transitioned into EPON resin. The tissue was embedded in molds containing fresh resin and polymerized for 2 days at 65 °C. Sections (0.5-μm thick) were stained with methylene blue to determine the area for thin sectioning (at 70 nm) with a diamond knife. Sections were placed onto formvar on 100-mesh copper grids and stained with aqueous uranyl acetate and lead citrate. The grids were examined using a HITACHI Transmission Electron Microscope HT7700.

**REAL-TIME POLYMERASE CHAIN REACTION ANALYSIS.** Total RNA was extracted using Trizol reagents (Thermo Fisher Scientific, 15596018), and complementary DNA (cDNA) was synthesized using StarScript II First-strand cDNA Synthesis Kit (GenStar, A212-10). Real-time polymerase chain reaction (PCR) was performed with the ChamQ Universal SYBR qPCR Master Mix (Vazyme Biotech Co, Q711-02/03). The sequences of primers used in this study can be found in Supplemental Table 1.

**MI SURGERY.** MI surgery was performed as previously described.[34] Briefly, adult mice aged 6 to 8 weeks were induced with tamoxifen (80 μg/g) by gavage for 2 weeks before MI injury. Adult $Wt1^{ERT2Cre}$, $Ccm2^{fl/fl}$, and $Ccm2^{fl/fl}$ mice were anesthetized with 1% isoflurane. The mice were placed in a left supine position on a heating pad (37 °C), and the heart was exposed at the fourth left intercostal space with thoracotomy. The pericardium was then opened, and the left coronary artery was permanently ligated with a 7-0 suture. Ligation was considered successful when the left ventricle became pale. The chest was then closed with 6-0 suture. Echocardiography was performed at 1 and 2 weeks after surgery. The mice were then sacrificed, and the hearts were subjected to histology using standard paraffin processing and staining procedures.

**ECHOCARDIOGRAPHY.** For echocardiographic assessment, animal preparation followed previous reports.[34] Briefly, adult mice were anesthetized with inhalation of isoflurane (2.5%-3.0%) using a nose cone. Mice were placed on a heat mat in the supine position to keep the body temperature around 37 °C. The chest hair was removed using hair removal gel cream. Warm acoustic gel was applied to the scan field as a coupling medium. Using a VisualSonics Vevo 2100 system and a 30-MHz transducer, M-mode images and real-time 2-dimensional B-mode cine loops of short- and long-axis views of the left ventricle were acquired for cardiac structure and function assessment. Transmitral inflow Doppler spectra and tissue Doppler were recorded in an apical 4-chamber view for diastolic function assessments. Echocardiographic images were analyzed using VevoLab software (3.2.0, VisualSonics Inc).

**STATISTICAL ANALYSIS.** Data are expressed as mean ± SEM. Between-group comparisons were done using unpaired Student's *t*-test (2 groups) and 2-way analysis of variance with Bonferroni test for multiple pairwise comparisons. The number of offspring from mouse mating was analyzed with the chi-square test. Analyses were done using GraphPad Prism statistical software (version 8.0.1 for Windows, GraphPad Software). A $P$ value $<0.05$ was considered statistically significant.

## RESULTS

**EPICARDIAL CCM2 IS REQUIRED FOR HEART DEVELOPMENT.** Previous studies have shown that Ccm signaling in endothelial cells regulates heart development.[24,25,35] To determine a potential role for Ccm in the epicardium during heart development, $Ccm2^{fl/fl}$ mice were crossed with the $Wt1^{GFPCre}$

knock-in mice to generate the $Wt1^{GFPCre}$;$Ccm2^{fl/fl}$ mice (thereafter, $Ccm2^{EPKO}$ mice) with specific deletion of the *Ccm2* gene in the epicardium.[29,36] Among 106 neonatal offspring from the genetic cross, only 1 live $Ccm2^{EPKO}$ mouse was observed, but it died by postpartum day 10 (Table 1). Timed mating studies showed that $Ccm2^{EPKO}$ embryos were observed at the expected Mendelian ratio up to E13.5, but the number of these embryos steadily declined as gestation progressed (Table 1). This suggests that Ccm2 expression is required in epicardial cells to support heart development. The compact myocardium in littermates grew continuously from E10.5 to E14.5 (Figures 1A to 1C). Histological analysis showed that there were no notable differences in the structure of the compact myocardium in the $Ccm2^{EPKO}$ hearts in comparison to that of littermate control mice (Ccm2$^{fl/fl}$ or $Wt1^{GFPCre}$;$Ccm2^{fl/+}$) at E10.5 (Figure 1A). Starting from E12.5, the compact myocardium was visibly thinner in the $Ccm2^{EPKO}$ hearts compared with that of control hearts (Figures 1B to 1D). This disruption in compact myocardium development coincided with the decreased number of live $Ccm2^{EPKO}$ embryos observed from E14.5 (Table 1). These data support the hypothesis that Ccm2 is crucial in epicardial cells to support compact myocardial development.

To determine whether the role of Ccm2 in epicardium is conserved among CCM complex proteins, we crossed $Wt1^{GFPCre}$ with $Ccm3^{fl/fl}$ mice to generate $Ccm3^{EPKO}$ mice. $Ccm3^{EPKO}$ mice were able to survive to late gestation stage and exhibited the expected ratio. Although $Ccm3^{EPKO}$ mice could be born alive, most of them did not survive beyond the weaning stage (Supplemental Table 2, Supplemental Figures 1A and 1B). Thinning of ventricle wall was detectable in E14.5 embryos, and severe myocardial thinning was observed in E16.5 embryos (Supplemental Figure 1). These findings suggest Ccm3 has similar roles in the epicardium to support cardiac development.

**CCM2 REGULATES EPICARDIAL CELL ADHESION, PROLIFERATION, AND MIGRATION IN VIVO.** To determine how loss of *Ccm2* affects the function of epicardium and heart development, we immunostained sections of embryos with an antibody against the epicardial marker Wt1.[37] Epicardial cells in the control hearts are generally circular and uniform in shape, and tightly attached to each other. In contrast, the Wt1$^+$ nuclei vary in size in the $Ccm2^{EPKO}$ mutants. Focal detachment of the epicardium from the myocardium and misaligned epicardial cells were observed in E12.5 $Ccm2^{EPKO}$ hearts, whereas epicardial cells in the control hearts were in continuous contact with the myocardium (Figure 2A). To assess whether loss of Ccm2 affected epicardial cell proliferation, double staining of Wt1 with either EdU pulse labeling or Ki67 immunostaining was performed. Mutant epicardial cells exhibited significantly reduced proliferative activity at E12.5 compared with control subjects (Figure 2B, Supplemental Figure 2A). Consistent with a thinner myocardium, EdU incorporation rate was significantly lower in the myocardium of the $Ccm2^{EPKO}$ embryos compared with their littermate control subjects (Supplemental Figure 2B). Epicardial cells arise from the proepicardium organ and migrate from the base to the apex of the heart to cover the entire surface by E11.5.[38] To assess the effect of *Ccm2* deficiency in epicardial cells on their migration and their capacity to cover the surface of myocardium, we performed wholemount staining of E10.5 hearts using MF-20 and anti-Wt1 antibodies. The 3D reconstructed images of the control hearts revealed complete coverage of the dorsal surface of the ventricle by Wt1$^+$ epicardial cells at E10.5. This is in stark contrast to only 60% coverage of the ventricular myocardium surface by Wt1$^+$ epicardial cells in the $Ccm2^{EPKO}$ hearts (Figure 2C). Aside from a role in the migration on myocardial surface from the base to apex of heart, epicardial cells also undergo endothelial-mesenchymal transition, migrate toward and penetrate the myocardium, and differentiate into epicardium derived cells (EPDCs) to support heart development. Cardiac fibroblast and coronary smooth muscle cells are 2 major types of EPDCs. Wt1 staining demonstrated that there are EPDCs start to penetrate into myocardium in E12.5 heart of control mice, whereas no penetrating epicardial cells were observed in the hearts of $Ccm2^{EPKO}$ littermates. In fact, the epicardial cells remained at a distance from the myocardium in the $Ccm2^{EPKO}$ hearts at this stage (Figure 2D). Immunostaining of the fibroblast marker, Pdgfrα showed remarkedly decreased expression in the $Ccm2^{EPKO}$ heart compared with control hearts

**TABLE 1 Offspring of $Ccm2^{fl/fl}$ X $Wt1^{GFPCre}$;$Ccm2^{fl/+}$ Matings at Various Developmental Stages**

| | Genotypes | | | | | | | |
|---|---|---|---|---|---|---|---|---|
| | E10.5 | E11.5 | E12.5 | E13.5 | E14.5 | E15.5 | E16.5-E18.5 | P10 |
| $Ccm2^{fl/+}$ | 5 | 12 | 47 | 19 | 13 | 11 | 24 | 36 |
| $Wt1^{GFPCre}$;$Ccm2^{fl/+}$ | 4 | 15 | 54 | 23 | 9 | 11 | 18 | 33 |
| $Ccm2^{fl/fl}$ | 4 | 14 | 53 | 21 | 16 | 10 | 13 | 36 |
| $Wt1^{GFPCre}$;$Ccm2^{fl/fl}$ | **6** | **13** | **34** | **14** | **7** | **6** | **4**[a] | **1**[b] |
| Total | 19 | 54 | 188 | 77 | 45 | 38 | 59 | 106 |

Values are age in years. Viability of $Wt1^{GFPCre}$;$Ccm2^{fl/fl}$ mice at different developmental stages. **Bold** values indicate to stress the number of mutant embryos. [a]$P < 0.05$. [b]$P < 0.001$, chi-square test.

**FIGURE 1 Epicardial-Specific Deletion of *Ccm2* Impairs Heart Development**

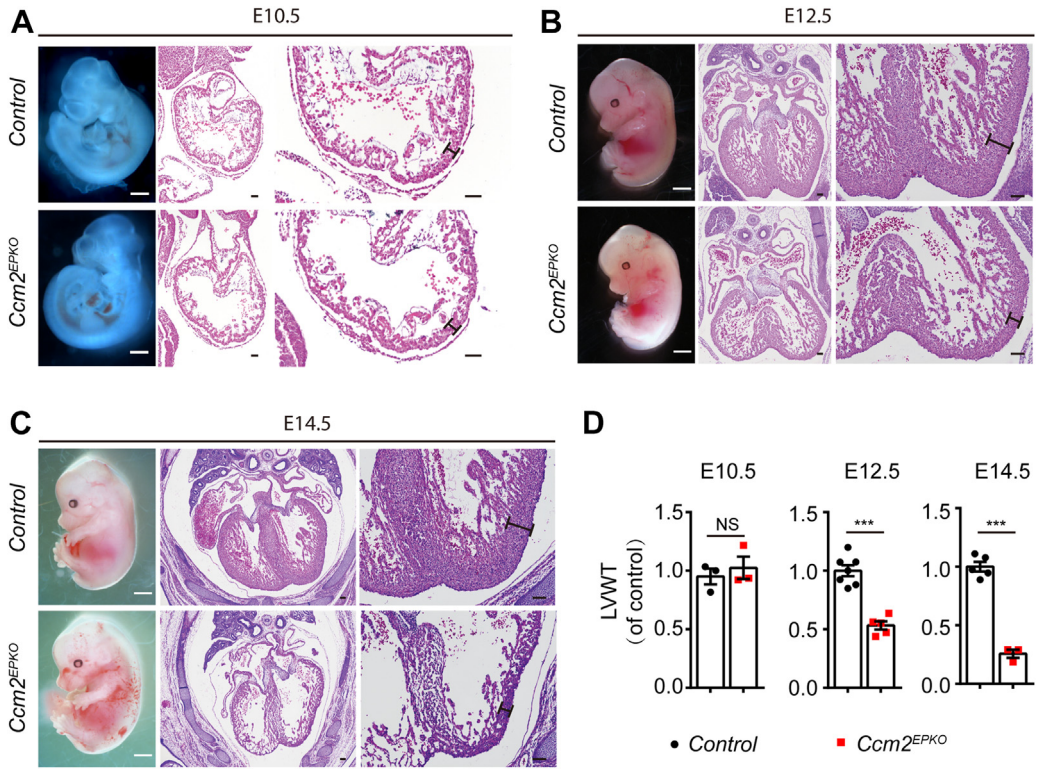


(A to C) Representative micrograph and hematoxylin and eosin staining of embryos at E10.5 (A), E12.5 (B), and E14.5 (C) showing decreased left ventricular wall thickness (LVWT) in the hearts of $Ccm2^{EPKO}$ mice at E12.5 and E14.5 (E = embryonic day). Micrograph: scale bar 0.2 mm. Hematoxylin and eosin staining: scale bar 100 μm. (D) Quantitation plots indicating the reduction of LVWT in the heart of $Ccm2^{EPKO}$ mice at E10.5 (n = 3), E12.5 (n = 5-7), and E14.5 (n = 3-5). Data in the quantitative plots are presented as mean ± SEM, and statistical significance was determined using an unpaired Student's *t*-test. ***$P < 0.001$. NS = not significant.

(Figure 2D). qPCR analysis confirmed the decreased expression of *Pdgfra, Pdgfrβ, Acta2,* and *Desmin* (Figure 2E). These results indicate a defective cell migration and differentiation in *Ccm2*-deficient epicardial cells.

**CCM2 REGULATES EPICARDIAL CELL PROLIFERATION, SPREADING, AND POLARITY EX VIVO.** To further understand the cell-autonomous role of Ccm2 in epicardial cells, we cultured epicardial cells from explanted E12.5 hearts of control and mutant mice. Gene expression analysis confirmed efficient deletion of *Ccm2* in epicardial cells from $Ccm2^{EPKO}$ hearts (Figure 3A). BrdU incorporation analysis showed that $Ccm2^{EPKO}$ epicardial cells have reduced proliferative activity (Figure 3B).

We next assessed epicardial cell spreading from the explanted control and mutant hearts via real-time imaging. We observed significantly increased epicardial cell outgrowth from the *Ccm2*-deficient hearts compared with the control subjects (Figure 3C) that was likely caused by the increased migration of the epicardial cells from these mutant hearts (Figure 3D). Considering that the $Ccm2^{EPKO}$ epithelial cells have reduced proliferative activity (Figure 3B), we hypothesized that the increased outgrowth area might be attributed to the effect of loss of *Ccm2* expression on epicardial cell size. It has been suggested that a migrating epicardium exhibits a leader/follower organization, whereby the cell areas of cells at the leading edge of a cellular outgrowth from an explant were largest, and this gradually decreased for the follower cells.[39] We stained the epicardial cell sheet with β-catenin and ZO-1 to mark cell boundaries and noted a remarkable increase in cell size for the migrating follower epicardial cells from $Ccm2^{EPKO}$ heart explants compared with that of littermate controls (Figures 3E and 3F). Closer examination of the spreading area of individual follower epicardial cells showed an ∼2-fold increase in cell size for cells

**FIGURE 2** **Epicardial-Specific Deletion of *Ccm2* Suppresses Epicardial Cell Adhesion, Proliferation, and Migration In Vivo**

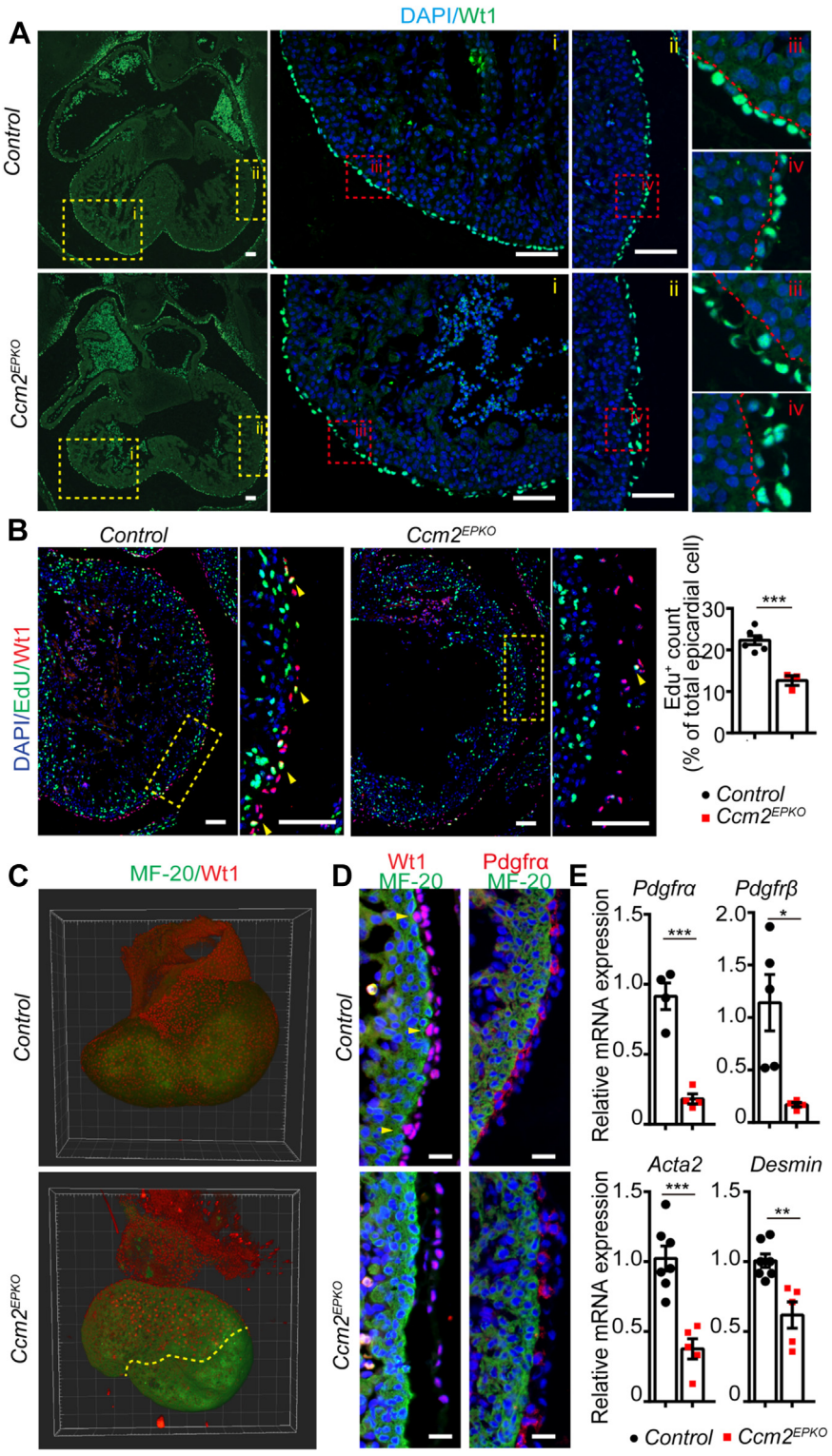


*Continued on the next page*

migrating out of the $Ccm2^{EPKO}$ heart explants compared with those from hearts of littermate control mice (Figure 3F). This increase correlated with a 2-fold decrease in the thickness of epicardial cells from $Ccm2^{EPKO}$ hearts (Figure 3G). These results suggest that *Ccm2* deficiency flattens epicardial cells to form a thinner cell sheet to compensate for the larger surface area in ex vivo culture. This in vitro observation closely resembles the phenotype of the endothelium in dilated CCM vessels.[40]

Directional cell migration requires polarized cytoskeleton, and Golgi apparatus are positioned forward facing at the leading edge of the cells.[32,41] In wild-type epicardial cells, immunostaining with a GM130, a Golgi marker, showed the Golgi apparatus were all forward facing to the leading edge, whereas in the $Ccm2^{EPKO}$ epicardial cells, the positions of Golgi apparatus were randomly distributed (Figure 4A). The calculated polarity index and the angular histogram of axial polarities relative to the spreading front edge confirmed that the $Ccm2^{EPKO}$ epicardial cells displayed randomized polarity patterns (Figures 4B to 4D). Thus, these results indicate that the Ccm2 is required in epicardial cells to maintain both cell shape and cell polarity, which are essential for directional cell migration.

**DELETION OF *CCM2* IN EPICARDIAL CELLS ALTERS THE EXPRESSION OF GENES RELATED TO CYTOSKELETAL AND MATRIX ORGANIZATION AND CELL MOTILITY.** To investigate the molecular mechanisms underlying the function of Ccm2 in epicardial cells, we profiled gene expression pattern in epicardial cells from E12.5 hearts of control and $Ccm2^{EPKO}$ embryos. Transcriptomic analysis demonstrated that the expression levels of 8994 transcripts were significantly different between epicardial cells from the $Ccm2^{EPKO}$ and littermate control hearts. The majority of altered genes were up-regulated in the mutants compared with control subjects, and only a small number were down-regulated. Among the most differentially expressed genes include known downstream transcriptional factors (*Klf2/4*), genes previously identified in cytoskeletal and matrix reorganization (*Krt14, Krt19, Lama4,* hyaluronan synthase 1 [*Has1*], *Hspg2, Vcan, Actg2,* and *Acta2*), and cytokines (*Bmp4* and *Bmp 10*) (Figures 5A and 5B). Gene ontology analysis confirmed the top gene sets altered after *Ccm2* deletion are those with a role in cytoskeletal organization, extracellular matrix assembly, and cell migration and motility (Figure 5C).

Keratins are major component of intermediate fibers.[42,43] Gene expression analysis confirmed significantly increased expression levels of keratin family genes in the $Ccm2^{EPKO}$ epicardial cells (Figure 6A). *Ccm2* deficiency also led to increased expression of genes encoding proteins involved in matrix assembly, including the laminin family genes, *Has1*, and *Hspg2*, a gene encoding perlecan (Figure 6A). Immunostaining of laminin showed increased laminin distribution between the *Ccm2*-deficient cell covered areas, whereas laminin was located intracellularly surrounding nucleus in control cells (Supplemental Figure 3). In addition, *Bmp4* and *Bmp10* expression were decreased in $Ccm2^{EPKO}$ epicardial cells (Figure 6A). Similar to that in endothelial cells, *Ccm2* deficiency in epicardial cells resulted in increased expression of *Klf2/4* (Figure 6A). The increased expression of *Klf2/4*, *Lama4,* and *Krt14* were also observed in *Ccm3* deficiency in epicardial cells (Supplemental Figure 4)

To determine whether the changed level of keratins affects cytoskeleton organization and contributes to altered epicardial cell morphology and cell motility, we used phalloidin and Krt19 antibody staining to examine the distribution of actin stress fibers and intermediate filaments, respectively. In the control epicardial cells, the actin filaments were abundant and typically aligned in the direction of cell migration, with fewer intermediate filaments observed. In *Ccm2*-deficient epicardial cells, however, Krt19 expression and presence of intermediate filaments were dramatically increased, whereas the actin stress fibers were markedly reduced (Figure 6B). We then used anti-α-tubulin and GM130 costaining to

**FIGURE 2 Continued**

(A) Wt1 immunostainings reveal the epicardium loosely adhered to the surface of myocardium in $Ccm2^{EPKO}$ mice at E12.5. Wt1 expression was detected in epicardium, as shown in 4 representative magnified regions. Scale bar: 100 μm. (B) EdU immunostainings and quantitative plots indicate the decreased proliferation in epicardial cells of $Ccm2^{EPKO}$ hearts at E12.5 (control, n = 6; $Ccm2^{EPKO}$, n = 3). Scale bar: 100 μm. (C) Costaining of Wt1 (epicardium marker, red) and MF20 (myocardium marker, green) on whole hearts reveals reduced overlap of the epicardium with the myocardium in $Ccm2^{EPKO}$ mice at E10.5 compared with that of control. (D) Coimmunostainings of Wt1 and Pdgfrα (fibroblast marker) with MF20, and staining of Snail (epithelial-mesenchymal transition marker) to correspondingly indicate the down-regulated transdifferentiation and endothelial-mesenchymal transition in $Ccm2^{EPKO}$ hearts at E12.5. Scale bar: 20 μm. (E) mRNA levels of *Pdgfra, Pdgfrβ, Acta2,* and *Desmin* (n = 4-7 for each group). Data in the quantitative plots are presented as mean ± SEM, and statistical significance was determined using unpaired Student's *t*-test. ***$P < 0.001$; **$P < 0.01$; *$P < 0.05$.

**FIGURE 3** ***Ccm2*** **Deficiency Suppresses Epicardial Cells Proliferation and Promotes Epicardial Cell Spreading Ex Vivo**

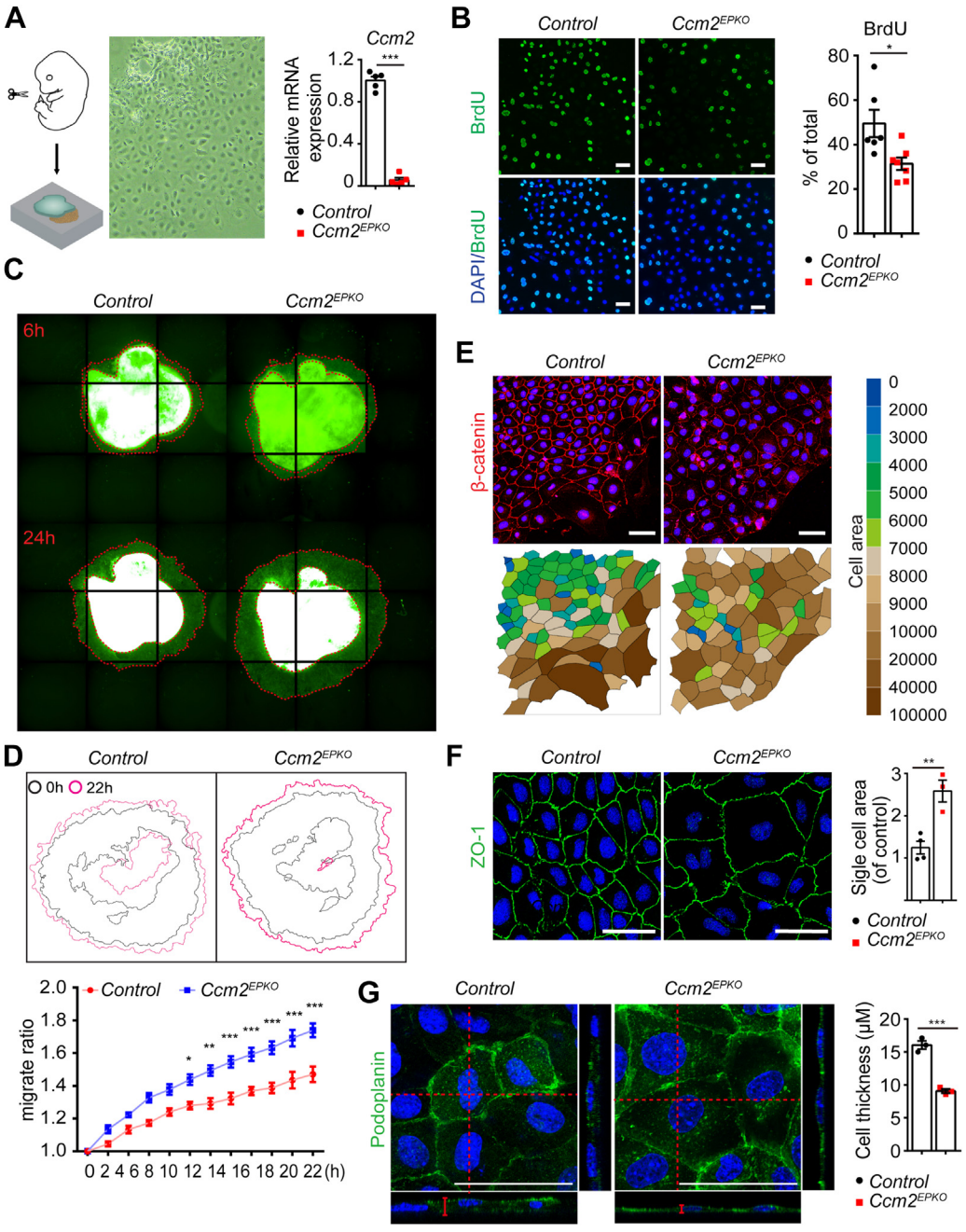


(A) Schematic representation (left) of ex vivo culture of epicardial cells from embryonic hearts and qPCR analysis (right) of *Ccm2* deletion efficiency in primary epicardial cells from E12.5 $Ccm2^{EPKO}$ hearts (n = 5 for each group). Brightfield image (middle) shows mouse epicardial cells in culture with characteristic epithelial morphology. (B) BrdU staining (left) and quantitation (right) of $BrdU^{+}$ epicardial cells to indicate the decreased proliferation in the epicardial cells of $Ccm2^{EPKO}$ mice at E12.5 (control, n = 6; $Ccm2^{EPKO}$, n = 7). Scale bar: 50 μm. (C) High-content images of epicardial cells as they spread outward from the heart. (D) Outline sketch and quantifications of the spreading ratio of epicardial cells after the removal of hearts from the dish, showing that epicardial cells from the $Ccm2^{EPKO}$ hearts spread faster compared with that of littermate controls (n = 3 for each group). (E) Immunostainings of β-catenin (red) and nuclei (DAPI, blue) (top) and color-coded cell area (bottom) in an expanding monolayer (heart at the top and leading edge at the bottom). Scale bar: 100 μm. (F) ZO-1 (green) staining and quantitation of single cell area (right) of epicardial cells to indicate the increased cell area of the epicardial cells from $Ccm2^{EPKO}$ hearts at E12.5 (control, n = 4; $Ccm2^{EPKO}$, n = 3). Scale bar: 100 μm. (G) Immunostainings of Podoplanin in epicardial cells from $Ccm2^{EPKO}$ and control hearts. The smaller horizontal strips at the bottom of each column are Z-sections to show cell thickness. Quantification analysis is shown on the right (n = 3 for each group). Scale bar: 100 μm. Data in the quantitative plots are presented as mean ± SEM, and significance was determined using unpaired Student's *t*-test, and 2-way analysis of variance followed by Bonferroni multiple comparisons test in (D). ***$P < 0.001$; **$P < 0.01$; *$P < 0.05$.

**FIGURE 4 Loss of Ccm2 Alters Cell Polarity Ex Vivo**

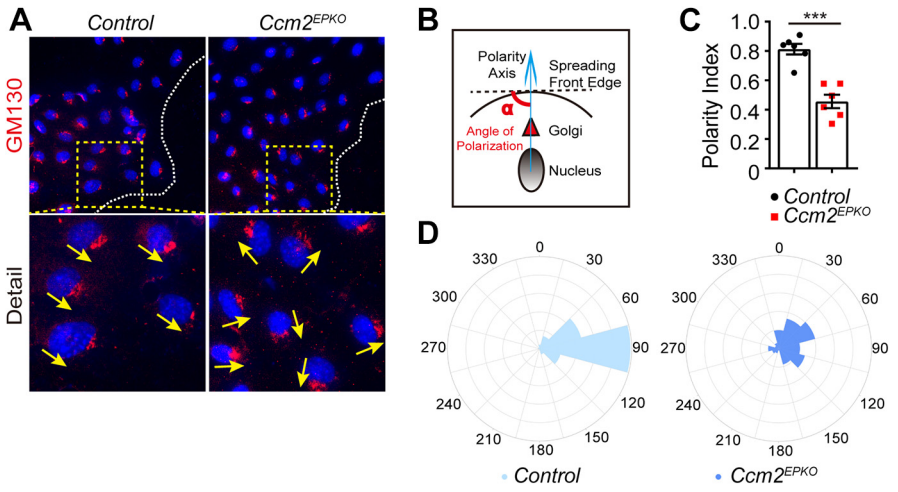


(A) Representative images of GM130 staining showing the location of Golgi and polarity angles of control and *Ccm2*-deficient epicardial cells. Scale bar: 20 μm. (B) The polarity axis of each cell was defined as the angle (α) between the edge and the cell polarity axis, defined by the vector drawn from the center of the cell nucleus to the center of the Golgi apparatus. The polarity index was calculated according to the formula and it was used as a measure for collective polarization. (C) Box plots of polarity index comparing control and *Ccm2*-deficient epicardial cells (n = 6 for each group). (D) Angular histograms showing the distribution of polarization angles of epicardial cells from control and *Ccm2*-deficient epicardial cells (n = 223 cells from 6 control mice; n = 192 cells, from 6 $Ccm2^{EPKO}$ mice). Data in the quantitative plots are presented as mean ± SEM, and significance was determined using unpaired Student's *t*-test. ***$P < 0.001$.

visualize microtubule structure and distribution. In control epicardial cells, abundant microtubules aligned with GM130-labelled Golgi in the leading side of the nucleus and in the direction of migration. In the *Ccm2*-deficient epicardial cells, α-tubulin staining signal was as strong as observed in the controls but displayed no structural organization (Figure 6C). These data suggest that Ccm2 expression in epicardial cells are required for the organization of actin stress fibers and microtubules, whereas the loss of Ccm2 led to the disassembly of these structures and disorganization of the intermediate filaments. These cytoskeletal changes were likely to be the cause of cell shape change and defect in cell migration observed in the $Ccm2^{EPKO}$ epicardial cells.

Next, we set to determine whether the changed expression of cytoskeletal and matrix genes and cell polarity can confer morphological/structural defects to the epicardium. Scanning electron microscopy images showed the epicardium of control hearts consisted of evenly distributed smooth epicardial cells, whereas the epicardial cells in the epicardium of *Ccm2*-deficient hearts were unevenly distributed. Furthermore, the epicardial cells in the *Ccm2*-deficient hearts displayed irregular cell shapes with increased extracellular matrix deposition and appeared to be detached from the myocardium (Figure 6D). As shown in the transmission electron microscopy images, epicardial cells are nicely attaching to myocardium in the control heart. The detachment of epicardial cells from myocardium is observed in the *Ccm2*-deficient heart, and the space between detached epicardial cells and myocardium were likely to be filled with excessive matrix components (Figure 6E).

RNA sequencing data revealed that *Bmp10* was the top down-regulated gene and *Has1* was the top up-regulated gene in *Ccm2*-deficient epicardial cells. To test whether they play a regulating role in epicardial cells, we treated epicardial cells from explanted hearts with recombinant BMP10 and found that the treatment prevented the increase of cell area observed in *Ccm2*-deficient epicardial cells (Supplemental Figure 5A). Has1 is an enzyme involved in hyaluronan synthesis. 4-MU has been shown to inhibit hyaluronan production both by modifying substrates for HAS and decreasing HAS gene expression.[44,45] When epicardial cells were treated with 4-MU, the average cell area was no longer increased in *Ccm2*-deficient cells (Supplemental Figure 5B). The expression levels of *Has1, Lama3, Lamb4, Krt14,* and *Krt19* were normalized or further reduced in treated *Ccm2*-deficient cells (Supplemental Figure 5C). Thus, the changes in the

**FIGURE 5** Transcriptomic Analysis of Epicardial Cells From *Ccm2*$^{EPKO}$ Hearts at E12.5

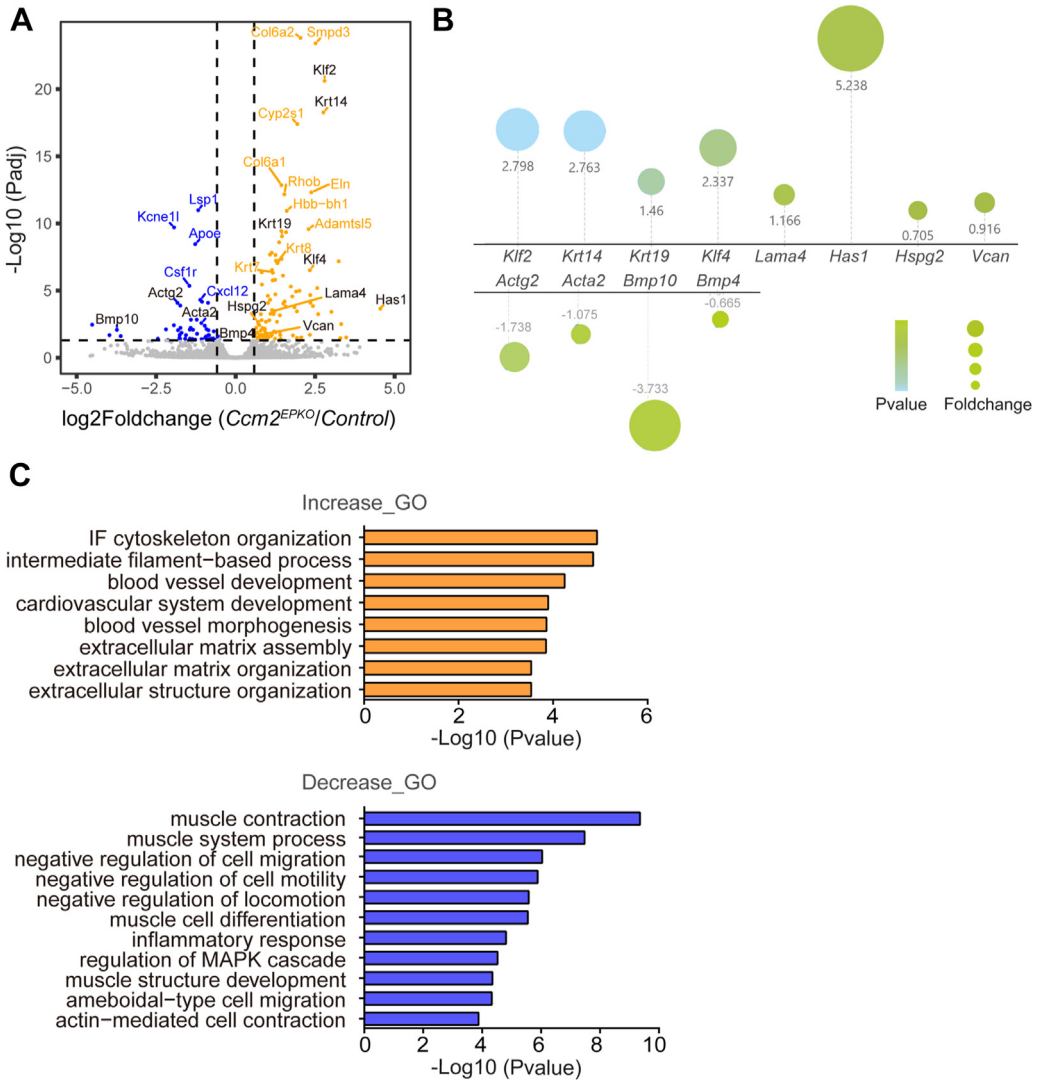


(A) Volcano plot shows *Krt14*, *Klf2*, and *Col6a2* are among the top up-regulated genes in *Ccm2*-deficient epicardial cells. (B) Bubble chart representation showing genes with increased and decreased expression, with the size of the bubble corresponding to fold change. (C) GO term analysis identified cytoskeleton and extracellular matrix as a top function that is up-regulated, and genes with functions relevant to cell motility and cell differentiation are among the top down-regulated genes in *Ccm2*-deficient epicardial cells at E12.5.

levels of both BMP and hyaluronan may affect the morphology and migration of epicardial cells.

**DELETION OF *CCM2* LED TO ALTERED CELL ORIENTATION AND MORPHOLOGY OF EPICARDIUM IN VIVO.** Having discovered the roles of Ccm2 in regulating epicardial cells behaviors ex vivo, we proceeded to determine whether these roles were conserved in vivo. Immunostainings showed increased expression of Krt19, laminin, and ColVI in the epicardium of E12.5 *Ccm2*$^{EPKO}$ hearts compared with that of control hearts (Figure 7A). Consistent with observations in cultured epicardial cells, GM130 staining analysis showed that the position of Golgi was disoriented in the *Ccm2*$^{EPKO}$ heart tissues. In control hearts, Golgi were typically located on the outer surface side of epicardial cells, whereas in *Ccm2*-deficient epicardial cells, they were observed to be randomly distributed around the nucleus (Figure 7B). Taken together, these studies confirm our in vitro findings, demonstrating that Ccm2 is required in epicardial cells to maintain the

**FIGURE 6** **Ccm2 Is Required for Cytoskeletal Organization and Cell Morphology Maintenance in Epicardial Cells**

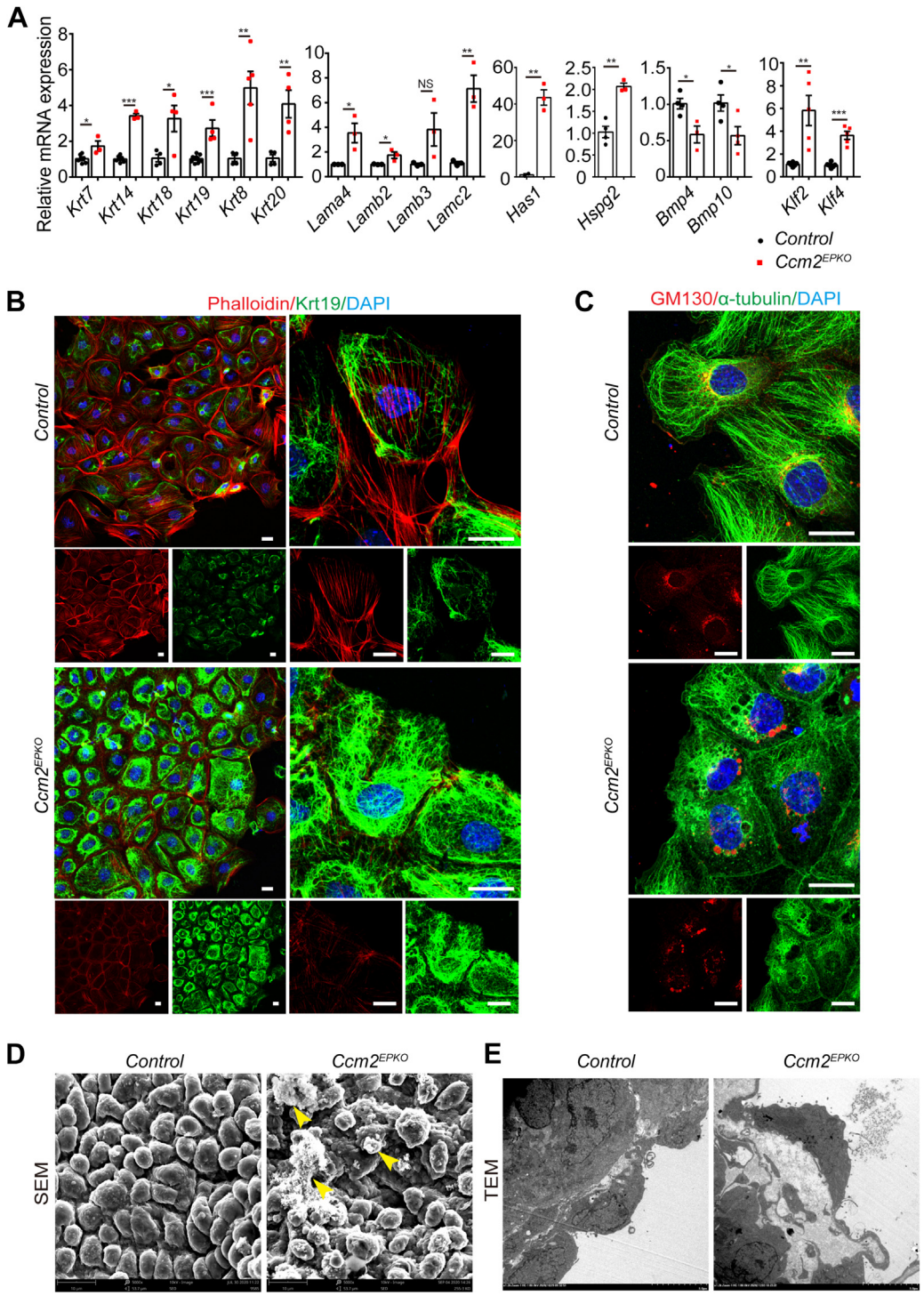


*Continued on the next page*

adhesion and integrity of epicardium via its regulation of cytoskeletal and matrix protein production as well as cell polarity.

**DELETION OF *CCM2* IN EPICARDIUM AGGRAVATES INJURY RECOVERY AFTER MYOCARDIUM INFARCTION.** It has been demonstrated that the epicardium plays essential roles in heart development, regeneration and injury recovery by supporting EPDC.[46,47] To elucidate whether Ccm2 in epicardial cells contributes to injury recovery following myocardium infarction, we crossed the $Ccm2^{fl/fl}$ mice with the inducible $Wt1^{ERT2Cre}$ mice[48,49] to generate the $Wt1^{ERT2Cre}$;$Ccm2^{fl/fl}$ (thereafter $Ccm2^{iEPKO}$) mice (Supplemental Figure 6A). *Ccm2* gene deletion was induced in these 6- to 8-week-old mice with tamoxifen injection. Myocardial infarction (MI) was performed after gene deletion (Supplemental Figures 6A to 6C). Cardiac performances were comparable before MI between $Ccm2^{iEPKO}$ and littermate control mice (**Figures 8A and 8B**). One and 2 weeks after MI, $Ccm2^{iEPKO}$ mice exhibited a significant depression of cardiac contractile performance (ejection fraction and fractional shortening) compared with that of sex-matched littermate control mice (**Figures 8A to 8C**). The changes in cardiac function did not affect the overall gross health of the mice because body weight of the mice lacking epicardial Ccm2 remained comparable to control subjects (**Figure 8D**). Wholemount bright-field images of hearts harvested at 14 days postinjury demonstrated that epicardial *Ccm2*-deficient hearts displayed a larger fibrous area at the pericardial surface compared with that in control mice after MI (**Figure 8E**). Serial histology images of coronary ligature-to-apex specimens from control hearts showed localized fibrosis in the infarct regions (**Figure 8F**), whereas *Ccm2*-deficient hearts showed increased fibrosis throughout the left ventricular free wall with loss of cardiomyocytes. Quantification of fibrotic scarring confirmed this observation (**Figure 8G**). Taken together, these observations demonstrate that Ccm2 in epicardium is not only required for heart development, but is also necessary for repair in adult heart after injury. Another question is whether Ccm2 is necessary for the maintenance of cardiac function. Echocardiographic analysis of $Ccm2^{iEPKO}$ mice 1.5 months after induced gene deletion did not reveal obvious defect (Supplemental Figure 6D); however, longer-term effects will require further investigation.

## DISCUSSION

Forward genetic studies in zebrafish found mutations in *ccm* genes in zebrafish cause a dilated heart phenotype.[23,26,27] Mouse genetic studies have established that endothelial *Ccm* genes are critical for cardiovascular development and CCM pathogenesis. From the early developmental stage, the heart consists of endocardium, myocardial, and epicardium. Due to failed lumen patterning of branchial arch arteries and dorsal aorta and embryonic lethality before E10, global endothelial Ccm2 knockout mice have been unable to provide conclusive information on the role of CCM2 during heart development. The cross of Ccm2 conditional allele with *Nfactc1*-Cre, which confers gene deletion in the endocardium, revealed the role of endocardial Ccm2 in maintaining cardiac jelly to facilitate early development of heart.[25] On the other hand, deletion of Ccm2 expression in myocardium with Nkx2.5-cre does not confer any heart defect.[26] It remained unclear whether epicardial-specific Ccm2 plays any role in cardiac development and function. In this study, we generated genetic murine models to specifically delete Ccm2 in the epicardium. The results of in vivo analysis and ex vivo culture of epicardial cells demonstrated a cell autonomous role of Ccm2 in epicardial cells, contributing to cardiac development and repair.

We found that the deletion of Ccm2 in epicardial cells affects the expression of cytoskeletal and matrix genes. The level of proteins encoded by these genes may participate in shaping the cell morphology, cell polarity, and adhesion activity. In vivo, *Ccm2* deficiency impairs cell adherence to myocardium and slows its migration rate to cover the myocardium. Changes in cytoskeletal organization and matrix

**FIGURE 6 Continued**

(A) mRNA level of cytokeratins (*Krt7, Krt8, Krt14, Krt18, Krt19, Krt20, Krt80*), *Laminins, Has1 and Hspg2*, bone morphogenetic proteins (*Bmp4* and *Bmp10*), and transcription factors (*Klf2 and Klf4*) (n = 3-8 for each group. Data are presented as mean ± SEM, and significance was determined using unpaired Student's *t*-test. ***$P < 0.001$; **$P < 0.01$; *$P < 0.05$.) (B) Representative confocal microscopy images showing increased cytokeratin-19 (Krt19) and decreased F-actin stress fiber (Phalloidin) in *Ccm2*-deficiency epicardial cells at E12.5. Scale bar: 20 μm. (C) Representative confocal microscopy images showing disrupted structure of α-tubulin and dislocated arrangement of Golgi apparatus (GM130) in *Ccm2*-deficiency epicardial cells at E12.5. Scale bar: 20 μm. (D) Representative scanning electron microscopy images of epithelium of $Ccm2^{EPKO}$ and control hearts. Arrowheads point to dislocated distribution of extracellular matrix. (n = 3 for each group). (E) Representative transmission electron microscopy images show epicardium loosely fit with myocardium in $Ccm2^{EPKO}$ heart. (n = 4 for each group).

**FIGURE 7 Deletion of *Ccm2* Leads to Increased Extracellular Matrix Production and Altered Cell Polarity**

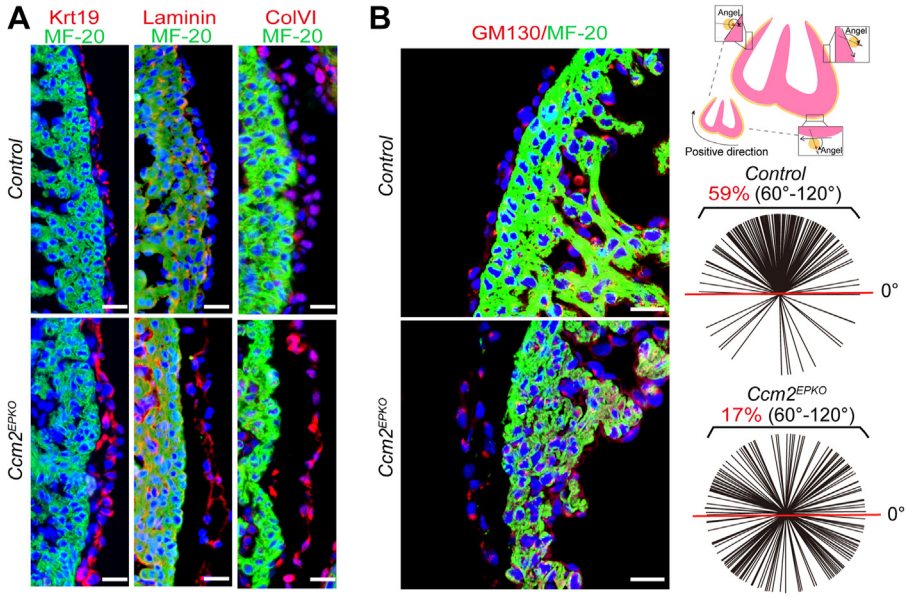


(A) Representative immunostaining images of Krt19, Laminin, and Collagen VI on heart sections show that cytoskeleton component Krt19, extracellular matrix component laminin, and Collagen VI significantly increase in *Ccm2*-deficient epicardium at E12.5 in vivo. Scale bar: 20 μm. (B) Coimmunostaining of MF20 and GM130 on heart sections of E12.5 $Ccm2^{EPKO}$ mice and quantification analysis shows dislocated arrangement of Golgi apparatus (GM130) in vivo. Scale bar: 20 μm. Schematic of GM130 and the angle measured between epicardial cells orientation and adjacent myocardial plain in order to determine positive direction (top panels) (n = 194 cells, from 4 control mice; n = 184 cells, from 4 $Ccm2^{EPKO}$ mice).

deposition may subsequently affect cell polarity organization that then, in turn, influences the migration of epicardial cells toward the myocardium and their differentiate into EPDC. In vitro, this misorganization of the cytoskeleton likely allows the epicardial cells to become more flatten. How the flattening phenotype of ex vivo cells correlated with the slowed surface coverage rate will require further investigation. It is possible that the combination of the changes in cell polarity, cytoskeleton protein abundance and organization, and the composition of matrix deposited between the epicardium and myocardium contributes to the migration and adhesion of epicardium in vivo. Moreover, the flattening of cultured epicardial cells resembles the flattening of endothelium and dilation of venous microvasculature in CCM patient and animals. In mouse embryos with endothelial-specific Ccm gene deletion, major arteries including dorsa aorta and branchial arch arteries are restricted, while the veins are dilated.[26,28,50] It is possible that the cytoskeletal and matrix mechanism are behind the differential endothelial phenotype between arterial and venous vessels and should be further explored in the vasculature of CCM model mice. Reshaping the cytoskeleton or the matrix-mediated interactions between endothelial cells and its neighboring cell types may help to alter cell morphology and correct the flattened endothelial cells and the dilated venules.

**STUDY LIMITATIONS.** Previous studies have found loss of *CCM1/2/3* gene in cultured endothelial cells increases stress fiber,[23,26] and loss of CCM3 affects Golgi assembly and cell polarity.[51] Here, in *Ccm2*-deficient epicardial cells, we observed reduced stress fibers, disoriented Golgi, and disrupted cell polarity, along with increased expression of cytokeratins and disorganized cytoskeletal structure. It is surprising that CCM2 deletion conferred an opposing effect on stress fiber organization seen in endothelial cells and epicardial cells. In endothelial cells, the balance of small GTPase RhoA and Cdc42 regulates stress fiber formation. The activation of these small GTPase needs to be analyzed in detail in epicardial cells. We speculate that the elevated gene expression of keratins upon Ccm2 deletion in epicardial cells might be an early event that confers a dominant effect on cytoskeletal structure and Golgi localization. The effect of CCM3 and its downstream effector STKs on

**FIGURE 8** **Induced Epicardial Deletion of *Ccm2* Aggravates Cardiac Function Loss and Fibrosis After Myocardial Infarction**

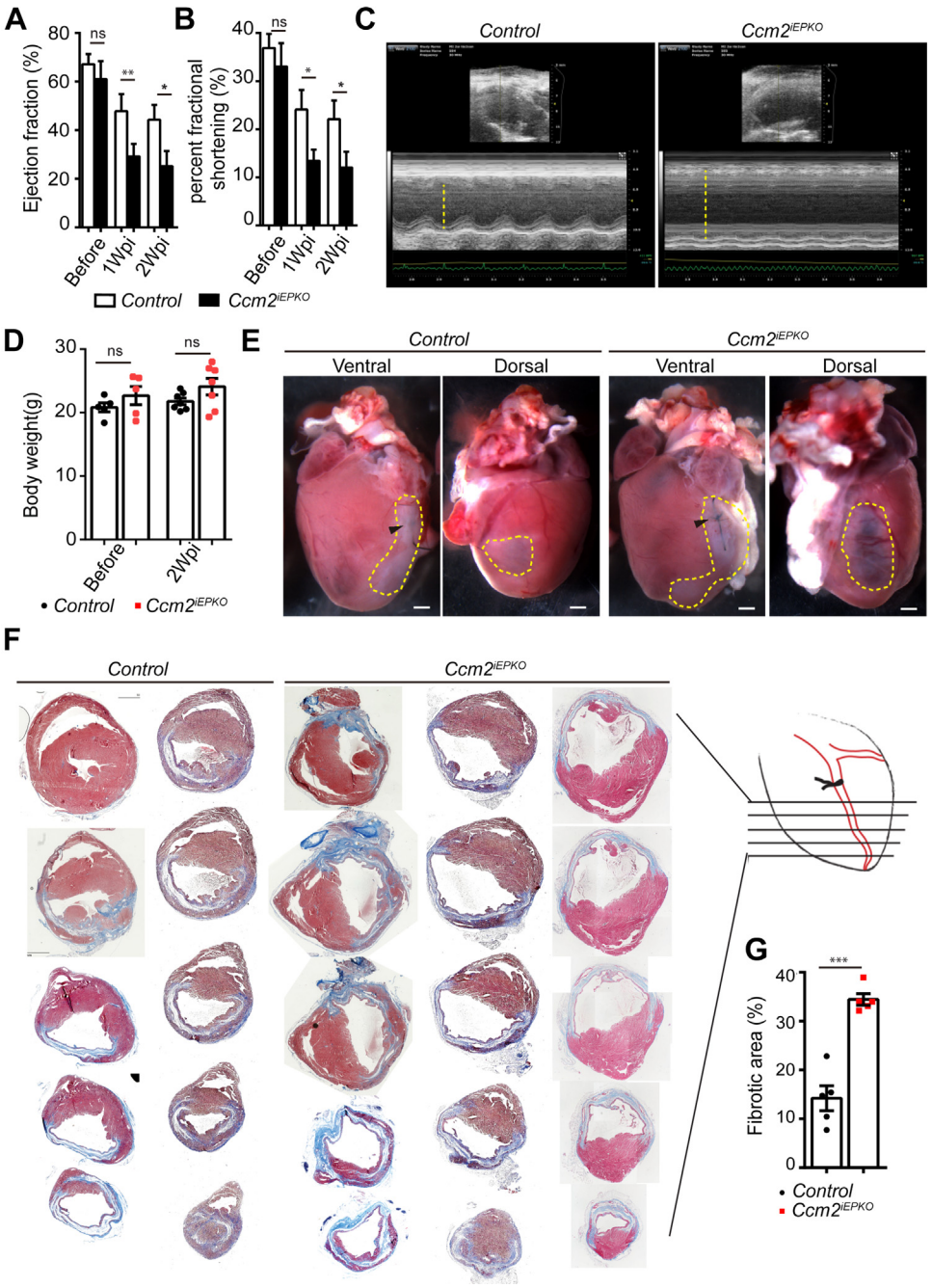


(A and B) Quantification of ejection fraction (A) and percent fraction shortening (B) reveal decreased heart function 1 and 2 weeks after myocardial infarction (Wpi) (n = 5 for each group). (C) Representative echocardiographic images reveal decreased cardiac contractility. (D) Quantification of body weight shows no significant change between *Ccm2*$^{iEPKO}$ and littermate control after myocardial infarction (n = 5-7 for each group). (E) Representative micrographs show aggravated myocardial necrosis in *Ccm2*$^{iEPKO}$ heart. Scale bar: 0.32 mm. (F and G) Masson's trichrome-stained serial sections (F) and quantification (G) of the fibrotic area relative to the myocardial area demonstrated a significant increase in scar formation in *Ccm2*$^{iEPKO}$ heart (n = 5 for each group). Data in the quantitative plots are presented as mean ± SEM, and significance was determined using unpaired Student's *t*-test, and 2-way analysis of variance followed by Bonferroni multiple comparisons test in A, B, and D. ***$P < 0.001$; **$P < 0.01$; *$P < 0.05$. NS = not significant.

Golgi assembly may cause additional cellular defects, which may, to a certain degree, explain why CCM3 mutations cause more severe disease burden. Further comparative studies of CCM diseases caused by CCM2 and CCM3 mutations will help to elucidate this hypothesis.

## CONCLUSIONS

Epicardium and epicardial-derived cells provided cytokines and differentiated cells to support heart development and regeneration.[47] Many molecular signals in epicardium have been shown to contribute to heart development. Here, we identified CCM2 as a cytoplasmic adaptor protein that regulates epicardial cell behaviors and indirectly affects the proliferation capacity and compaction of the developing myocardium, as well as the repair of injured myocardium in adult hearts. RNA-seq analysis also found that Ccm2 deficiency affects the expression of cytokines, such as the down-regulation of Bmp4 and Bmp10 expression. In ex vivo culture, adding back BMP10 can normalize epicardial cell morphology. Epicardial Ccm2 may play its roles in cardiac development via multiple mechanisms. Two major cell types derived from epicardial cells are fibroblast and smooth muscle cells, with smooth muscle cells contributing to the maturation of coronary vessels. The majority of $Ccm2^{EPKO}$ embryos die before E15.5. For the few embryos that survive past E15.5, the myocardium is extremely thin and very few coronary vessels were present (data not shown). Thus, it is uncertain whether Ccm2 deletion in epicardial cells can directly affect coronary vessel formation. Our data shows that Ccm3 deletion in epicardial cells causes similar cardiac development defects. However, the detailed roles and mechanisms of the other known CCM signaling molecules, Ccm1, Ccm3 and their known downstream effectors, in epicardial cells and in heart development will require further investigation. Together with previous studies, we conclude that Ccm2 functions in both endocardial and epicardial cells to support cardiac development and injury repair.

**ACKNOWLEDGMENTS** The authors thank Fei Wang and Shuxu Dong for the technical support of EM, and Guangmao Wen for the support of mouse colony maintenance. The authors also thank Jisheng Yang and Li Li for advice on histology techniques.

## FUNDING SUPPORT AND AUTHOR DISCLOSURES

The project is supported by funding from the National Key Research and Development Program of China (grants 2019YFA0802003 to Dr Zheng), National Natural Science Foundation of China grants 82170300 (to Dr Zheng), and National Health and Medical Research Council (1158997, 1158998) (to Dr Liu). The authors have reported that they have no relationships relevant to the contents of this paper to disclose.

**ADDRESS FOR CORRESPONDENCE:** Dr Xiangjian Zheng, Department of Pharmacology and Tianjin Key Laboratory of Inflammation Biology, School of Basic Medical Sciences, Tianjin Medical University, No.22 Qi Xiang Tai Road, Tianjin 300070, China. E-mail: xzheng@tmu.edu.cn.

## PERSPECTIVES

**COMPETENCY IN MEDICAL KNOWLEDGE:** CCM2 is a disease gene associated with cerebral cavernous malformation. Recent studies have revealed its importance in cardiac and vascular development. Using cell-type specific genetic tools and explant culture of the embryonic heart, our data show the absence of CCM2 in the epicardium impairs heart development and recovery after MI. This highlights the role of CCM2 in heart regeneration and suggests potential therapeutic strategies for improving cardiac recovery after injury.

**TRANSLATIONAL OUTLOOK:** The role of epicardial CCM2 in heart development and injury recovery following heart attacks opens new possibilities for translational research and therapeutic strategies for heart disease. Our data suggest that normalizing the extracellular matrix, manipulating gene expression to target the cytoskeletal network, and providing appropriate growth factors represent potential approaches that can enhance heart regeneration and recovery post-MI.

## REFERENCES

**1.** Katz D, Gavin MC. Stable ischemic heart disease. *Ann Intern Med*. 2019;171:ITC17–ITC32.

**2.** Nowbar AN, Gitto M, Howard JP, Francis DP, Al-Lamee R. Mortality from ischemic heart disease. *Circ Cardiovasc Qual Outcomes*. 2019;12:e005375.

**3.** Smits AM, Dronkers E, Goumans MJ. The epicardium as a source of multipotent adult cardiac progenitor cells: their origin, role and fate. *Pharmacol Res*. 2018;127:129–140.

**4.** Cao J, Poss KD. The epicardium as a hub for heart regeneration. *Nat Rev Cardiol*. 2018;15:631–647.

**5.** Quijada P, Trembley MA, Small EM. The role of the epicardium during heart development and repair. *Circ Res*. 2020;126:377–394.

**6.** von Gise A, Pu WT. Endocardial and epicardial epithelial to mesenchymal transitions in heart development and disease. *Circ Res*. 2012;110:1628–1645.

**7.** Streef TJ, Smits AM. Epicardial contribution to the developing and injured heart: exploring the cellular composition of the epicardium. *Front Cardiovasc Med*. 2021;8:750243.

**8.** Bax NA, van Oorschot AA, Maas S, et al. In vitro epithelial-to-mesenchymal transformation in human adult epicardial cells is regulated by TGFbeta-signaling and WT1. *Basic Res Cardiol*. 2011;106:829–847.

**9.** Martinez-Estrada OM, Lettice LA, Essafi A, et al. Wt1 is required for cardiovascular progenitor cell formation through transcriptional control of Snail and E-cadherin. *Nat Genet*. 2010;42:89–93.

**10.** von Gise A, Zhou B, Honor LB, Ma Q, Petryk A, Pu WT. WT1 regulates epicardial epithelial to mesenchymal transition through beta-catenin and retinoic acid signaling pathways. *Dev Biol*. 2011;356:421–431.

**11.** Wang S, Yu J, Jones JW, et al. Retinoic acid signaling promotes the cytoskeletal rearrangement of embryonic epicardial cells. *FASEB J*. 2018;32:3765–3781.

**12.** Lavine KJ, Yu K, White AC, et al. Endocardial and epicardial derived FGF signals regulate myocardial proliferation and differentiation in vivo. *Dev Cell*. 2005;8:85–95.

**13.** Wang J, Liu S, Heallen T, Martin JF. The Hippo pathway in the heart: pivotal roles in development, disease, and regeneration. *Nat Rev Cardiol*. 2018;15:672–684.

**14.** Singh A, Ramesh S, Cibi DM, et al. Hippo signaling mediators Yap and Taz are required in the epicardium for coronary vasculature development. *Cell Rep*. 2016;15:1384–1393.

**15.** Li J, Miao L, Zhao C, et al. CDC42 is required for epicardial and pro-epicardial development by mediating FGF receptor trafficking to the plasma membrane. *Development*. 2017;144:1635–1647.

**16.** Ma X, Sung DC, Yang Y, Wakabayashi Y, Adelstein RS. Nonmuscle myosin IIB regulates epicardial integrity and epicardium-derived mesenchymal cell maturation. *J Cell Sci*. 2017;130:2696–2706.

**17.** Fischer A, Zalvide J, Faurobert E, Albiges-Rizo C, Tournier-Lasserve E. Cerebral cavernous malformations: from CCM genes to endothelial cell homeostasis. *Trends Mol Med*. 2013;19:302–308.

**18.** Vernooij MW, Ikram MA, Tanghe HL, et al. Incidental findings on brain MRI in the general population. *N Engl J Med*. 2007;357:1821–1828.

**19.** Snellings DA, Hong CC, Ren AA, et al. Cerebral cavernous malformation: from mechanism to therapy. *Circ Res*. 2021;129:195–215.

**20.** Sahoo T, Johnson EW, Thomas JW, et al. Mutations in the gene encoding KRIT1, a Krev-1/rap1a binding protein, cause cerebral cavernous malformations (CCM1). *Hum Mol Genet*. 1999;8:2325–2333.

**21.** Gunel M, Awad IA, Finberg K, et al. A founder mutation as a cause of cerebral cavernous malformation in Hispanic Americans. *N Engl J Med*. 1996;334:946–951.

**22.** Denier C, Goutagny S, Labauge P, et al. Mutations within the MGC4607 gene cause cerebral cavernous malformations. *Am J Hum Genet*. 2004;74:326–337.

**23.** Zheng X, Xu C, Di Lorenzo A, et al. CCM3 signaling through sterile 20-like kinases plays an essential role during zebrafish cardiovascular development and cerebral cavernous malformations. *J Clin Invest*. 2010;120:2795–2804.

**24.** Mably JD, Chuang LP, Serluca FC, Mohideen MA, Chen JN, Fishman MC. santa and valentine pattern concentric growth of cardiac myocardium in the zebrafish. *Development (Cambridge, England)*. 2006;133:3139–3146.

**25.** Zhou Z, Rawnsley DR, Goddard LM, et al. The cerebral cavernous malformation pathway controls cardiac development via regulation of endocardial MEKK3 signaling and KLF expression. *Dev Cell*. 2015;32:168–180.

**26.** Whitehead KJ, Chan AC, Navankasattusas S, et al. The cerebral cavernous malformation signaling pathway promotes vascular integrity via Rho GTPases. *Nat Med*. 2009;15:177–184.

**27.** Zheng X, Xu C, Smith AO, et al. Dynamic regulation of the cerebral cavernous malformation pathway controls vascular stability and growth. *Dev Cell*. 2012;23:342–355.

**28.** Chan AC, Drakos SG, Ruiz OE, et al. Mutations in 2 distinct genetic pathways result in cerebral cavernous malformations in mice. *J Clin Invest*. 2011;121:1871–1881.

**29.** Zhou B, Ma Q, Rajagopal S, et al. Epicardial progenitors contribute to the cardiomyocyte lineage in the developing heart. *Nature*. 2008;454:109–113.

**30.** National Research Council of the National Academies. *Guide for the Care and Use of Laboratory Animals*. National Academies Press; 2011.

**31.** Liu Y, Antonyak M, Peng X. Visualization of mouse embryo angiogenesis by fluorescence-based staining. *Methods Mol Biol*. 2012;843:79–85.

**32.** Carvalho JR, Fortunato IC, Fonseca CG, et al. Non-canonical Wnt signaling regulates junctional mechanocoupling during angiogenic collective cell migration. *Elife*. 2019;8.

**33.** Jiang X, Hu J, Wu Z, et al. Protein phosphatase 2A mediates YAP activation in endothelial cells upon VEGF stimulation and matrix stiffness. *Front Cell Dev Biol*. 2021;9:675562.

**34.** Wu Y, Zhou L, Liu H, et al. LRP6 downregulation promotes cardiomyocyte proliferation and heart regeneration. *Cell Res*. 2021;31:450–462.

**35.** Mably JD, Mohideen MA, Burns CG, Chen JN, Fishman MC. heart of glass regulates the concentric growth of the heart in zebrafish. *Curr Biol*. 2003;13:2138–2147.

**36.** Zhou B, Pu WT. Genetic Cre-loxP assessment of epicardial cell fate using Wt1-driven Cre alleles. *Circ Res*. 2012;111:e276–e280.

**37.** Zeng B, Ren XF, Cao F, Zhou XY, Zhang J. Developmental patterns and characteristics of epicardial cell markers Tbx18 and Wt1 in murine embryonic heart. *J Biomed Sci*. 2011;18:67.

**38.** Poelmann RE, Gittenberger-de Groot AC. Cardiac birth defects. *Differentiation*. 2012;84:1–3.

**39.** Uroz M, Garcia-Puig A, Tekeli I, et al. Traction forces at the cytokinetic ring regulate cell division and polyploidy in the migrating zebrafish epicardium. *Nat Mater*. 2019;18:1015–1023.

**40.** Tu J, Stoodley MA, Morgan MK, Storer KP. Ultrastructural characteristics of hemorrhagic, nonhemorrhagic, and recurrent cavernous malformations. *J Neurosurg*. 2005;103:903–909.

**41.** Cao J, Wang J, Jackman CP, et al. Tension creates an endoreplication wavefront that leads regeneration of epicardial tissue. *Dev Cell*. 2017;42:600–615.e4.

**42.** Pegoraro AF, Janmey P, Weitz DA. Mechanical properties of the cytoskeleton and cells. *Cold Spring Harb Perspect Biol*. 2017;9(11):a022038.

**43.** Yoon S, Leube RE. Keratin intermediate filaments: intermediaries of epithelial cell migration. *Essays Biochem*. 2019;63:521–533.

**44.** Kultti A, Pasonen-Seppanen S, Jauhiainen M, et al. 4-methylumbelliferone inhibits hyaluronan synthesis by depletion of cellular UDP-glucuronic acid and downregulation of hyaluronan synthase 2 and 3. *Exp Cell Res*. 2009;315:1914–1923.

**45.** Li W, Yang S, Xu P, et al. SARS-CoV-2 RNA elements share human sequence identity and upregulate hyaluronan via NamiRNA-enhancer network. *EBioMedicine*. 2022;76:103861.

**46.** Ramjee V, Li D, Manderfield LJ, et al. Epicardial YAP/TAZ orchestrate an immunosuppressive response following myocardial infarction. *J Clin Invest*. 2017;127:899–911.

**47.** Simões FC, Riley PR. The ontogeny, activation and function of the epicardium during heart development and regeneration. *Development*. 2018;145:dev155994.

**48.** Zhou B, Honor LB, He H, et al. Adult mouse epicardium modulates myocardial injury by secreting paracrine factors. *J Clin Invest*. 2011;121:1894–1904.

**49.** Zhou B, Pu WT. Epicardial epithelial-to-mesenchymal transition in injured heart. *J Cell Mol Med*. 2011;15:2781–2783.

**50.** Kleaveland B, Zheng X, Liu JJ, et al. Regulation of cardiovascular development and integrity by the heart of glass-cerebral cavernous malformation protein pathway. *Nat Med*. 2009;15:169–176.

**51.** Fidalgo M, Fraile M, Pires A, Force T, Pombo C, Zalvide J. CCM3/PDCD10 stabilizes GCKIII proteins to promote Golgi assembly and cell orientation. *J Cell Sci*. 2010;123:1274–1284.

**KEY WORDS** CCM, cytoskeleton, ECM, epicardium, myocardial infarction, polarity

**APPENDIX** For supplemental tables and figures, please see the online version of this paper.